JOURNAL OF CATALYSIS **160,** 205–213 (1996)
ARTICLE NO. 0139

# *In Situ* Controlled Promotion of Catalyst Surfaces via NEMCA: The Effect of Na on the Ag-Catalyzed Ethylene Epoxidation in the Presence of Chlorine Moderators

Ch. Karavasilis, S. Bebelis, and C. G. Vayenas

*Department of Chemical Engineering, University of Patras, GR-26500 Patras, Greece*

Received May 8, 1995; revised November 20, 1995; accepted January 18, 1996

**The effect of non-Faradaic electrochemical modification of catalytic activity, or *in situ* controlled promotion, was investigated during ethylene epoxidation on Ag films deposited on $\beta''$-$Al_2O_3$, a $Na^+$ conductor, at temperatures 240 to 280°C and 500 kPa total pressure in the presence of chlorinated hydrocarbon moderators. The $\beta''$-$Al_2O_3$ support permits controlled and reversible potentiostatic introduction of various levels of sodium on the Ag catalyst surface. It was found that sodium coverages up to 0.03 enhance the rate of epoxidation without affecting significantly the rate of complete oxidation. The promotion index of sodium for ethylene epoxidation is up to 40. Maximum selectivity to ethylene oxide (88%) is obtained for $\theta_{Na} = 0.03$ and 1 ppm dichloroethane. The promoting and synergistic action of sodium and chlorine is discussed on the basis of previous *in situ* controlled promotion studies and the prevailing ideas about the mechanism of ethylene epoxidation.** 

## INTRODUCTION

The Ag-catalyzed epoxidation of ethylene, a reaction of great technological importance, is one of the most challenging and thoroughly studied catalytic systems (1–4). Extensive research has been carried out during the past 30 years aimed at both enhancing the industrial selectivity to ethylene oxide and improving the fundamental understanding of the underlying catalytic chemistry. Work prior to 1987 has been reviewed by van Santen and Kuipers (4).

Most industrial reactors operate currently with a selectivity in excess of 80% (4). The catalyst consists of reduced Ag particles dispersed on $\alpha$-$Al_2O_3$. Alkalis are added to the catalyst as promoters and chlorinated hydrocarbons are added at the ppm level to the feed as moderators. The role of promoters and moderators is to a significant extent synergistic and has been studied intensively in recent years (5–12). Despite substantial progress in this area no unanimous conclusions have yet been reached.

Regarding the catalytically active surface oxygen species, it is currently generally accepted that it is atomic oxygen (4), as shown conclusively by the work of Lambert and coworkers in the early and mid-1980s (13, 14). The presence of subsurface oxygen (15–17) is a necessary condition for obtaining high selectivity to ethylene oxide (4, 13, 18), while molecularly adsorbed oxygen has been shown to be a spectator species (4, 13, 14, 19). Product selectivity is strongly influenced by the binding state of atomic oxygen (4, 13). Weakly bound, electrophilic oxygen leads to epoxide by reaction with the $\pi$-orbitals of chemisorbed ethylene (4, 13, 20–22). Strongly bound, bridging, oxygen attacks preferentially C–H bonds and leads to nonselective oxidation (4, 13, 20–22). The effect of promoters and moderators on the coverage and binding state of adsorbed atomic oxygen is still the focal point of numerous studies (4–12).

The effect of non-Faradaic electrochemical modification of catalytic activity (NEMCA) (23) has been described in recent years for more than 30 catalytic reactions on Pt, Pd, Rh, Ag, Au, $IrO_2$, and Ni catalysts interfaced with $O^{2-}$, $Na^+$, $F^-$, and $H^+$ conducting solid electrolytes (24–37) and more recently with aqueous solutions (38). The NEMCA literature has been reviewed recently (34–37). The effect has been shown to be due to an electrochemically induced and controlled backspillover of promoting species ($O^{\delta-}$, $Na^{\delta+}$, etc.) from the solid electrolyte onto the catalyst surface (25, 34, 39) as recently confirmed by XPS (39). The NEMCA-induced reversible change in catalytic rate is up to $3 \times 10^5$ higher than the rate of ion supply (24) and up to 100 times larger than the open-circuit rate (27). More recently even higher rate enhancement values have been obtained for the NO reduction by ethylene (31). The importance of NEMCA in catalysis (40) and electrochemistry (41) has been discussed recently.

Previous NEMCA studies utilizing $\beta''$-$Al_2O_3$, a $Na^+$ conductor, as the solid electrolyte and promoter donor, were limited to Pt catalysts (28, 29, 31, 33). The present work is the first NEMCA study utilizing $\beta''$-$Al_2O_3$ to promote a catalytic reaction on Ag. A useful parameter for quantifying NEMCA and the role of promoters is the promotion index $P_i$ (27, 29) defined from

$$P_i = \frac{\Delta r / r_o}{\Delta \theta_i}, \qquad [1]$$



0021-9517/96 $18.00

where $\Delta r$ is the promotion-induced catalytic rate increase, $r_0$ is the open-circuit (unpromoted) catalytic rate, and $\theta_i$ is the coverage of the promoting species, i.e., $Na^{\delta+}$ in the present case. When $P_i > 0$, then the ion under consideration has a promoting effect on the catalytic rate and can cause NEMCA. When $P_i < 0$, then it has a poisoning effect on the rate. In this case $-P_i$ equals the "toxicity" of the atom or ion, defined by Barbier and co-workers (42). When the ion just blocks surface sites it is $P_i = -1$. Previous NEMCA studies with $\beta''$-$Al_2O_3$ have given $P_{Na}$ values up to 250 (28, 29, 31, 33) which show strong electronic interactions.

The ethylene epoxidation on Ag was one of the first reactions found to exhibit non-Faradaic electrochemical promotion with $O^2$-conducting solid electrolytes (43–45). In a very recent study (46) utilizing YSZ solid electrolyte as the $O^{2-}$ donor, high operating pressure (500 kPa), low operating temperature (250°C), and addition of chlorinated hydrocarbon moderators, ethylene oxide selectivity up to 78% was obtained.

Similar operating conditions, close to those of industrial practice, are used in the present work, which examines *in situ* the promotional effect of sodium and chlorine on ethylene epoxidation.

## EXPERIMENTAL

The experimental apparatus utilizing on-line gas chromatography, mass spectrometry, IR spectroscopy, and an electrochemical oxygen analyzer for reactant and product analysis has been described in previous papers (45–47).

Reactants were Messer Griesheim or L′ Air Liquide certified standards of $C_2H_4$ in He, $O_2$ in He, and 1,2-$C_2H_4Cl_2$ in He. They could be further diluted in ultrapure 99.999% He.

The gas chromatographic analysis was carried out using a Shimadzu 14A gas chromatograph with a TC and an FI detector and a Perkin-Elmer LCI-100 computing integrator. A Porapak N packed column (80/100, $8' \times \frac{1}{8}''$) was used to separate $O_2$, $CO_2$, and $C_2H_4$ at 70°C, as well as $C_2H_4O$ and $H_2O$ at 150°C. The $O_2$ concentration was also measured using a Molecular Sieve 5A packed column (80/100, $8' \times \frac{1}{8}''$) at 70°C and was continuously monitored in the exit stream by means of a Teledyne 326 RA oxygen electrochemical analyzer. The concentration of $CO_2$ in the product stream was also monitored using on-line IR spectroscopy (Foxboro 973 Miran analyzer). A Balzers QMG 311 mass spectrometer was also used to follow rate transients. The carbon mass balance closure in all runs was better than 2%. No coking of the catalyst was detected. The only detectable products were $CO_2$, $C_2H_4O$, and $H_2O$. Contrary to the parallel study of ethylene epoxidation on Ag deposited on $Y_2O_3$-stabilized $ZrO_2$ (46), the rate of acetaldehyde formation was negligible over all conditions. The inlet concentration of 1,2-$C_2H_4Cl_2$ in the gas phase was computed by measuring the individual flow rate of each certified gas mixture supplied to the reactor. Care was taken so that the pressure just before the mixing point was the same for each individual gas stream, in order to avoid any errors in the calculation of the inlet 1,2-$C_2H_4Cl_2$ concentration. Also care was taken to maintain a dry stream of air through the reactor, when not in use, in order to minimize the interaction of $\beta''$-$Al_2O_3$ with moisture which can lead to significant proton incorporation in the lattice.

An important experimental problem which we encountered in absence of gas-phase dichloroethane was the reaction of $CO_2$ with the sodium of the $\beta''$-$Al_2O_3$ support to form $Na_2CO_3$ on the $\beta''$-$Al_2O_3$ surface. This results in poor closure of the carbon mass balance and may lead to significant errors in computing the selectivity. Fortunately, the problem disappears completely in the presence of even trace amounts of dichloroethane, since NaCl rather than $Na_2CO_3$ formation is thermodynamically favored (48). All results reported here were obtained in presence of dichloroethane.

The reaction was carried out in a single pellet reactor (34, 49, 50) (Fig. 1). A tubular element of $\beta''$-$Al_2O_3$ (10 mm od, 1 mm thickness, 20 mm length) was suspended in the interior of a quartz tube of 30 $cm^3$ volume, surrounded by the reaction mixture under a total pressure of 500 kPa. The reactor was pressurized by throttling the outlet stream via a needle valve and the pressure in the reactor was measured via a mechanical pressure gauge. The catalyst-working electrode was a porous silver film deposited on the outer surface of the $\beta''$-$Al_2O_3$ tubular element using thin coatings of a Ag solution in butyl acetate (GC electronics, silver print

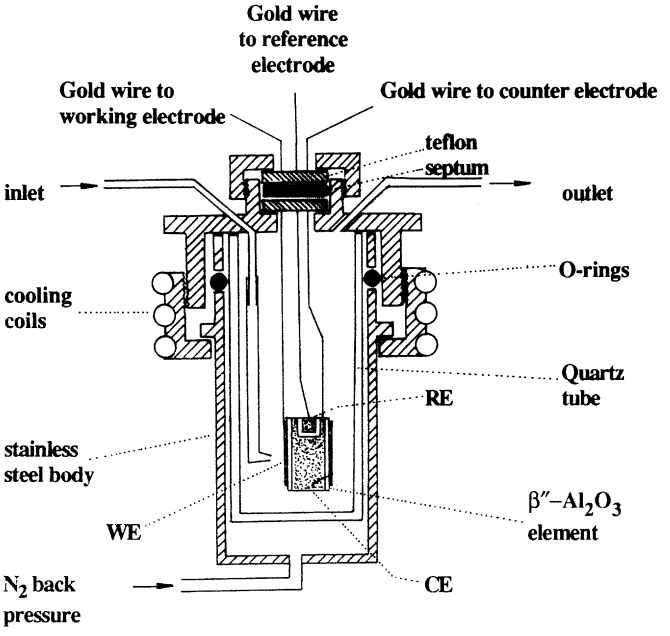


**FIG. 1.** Cross-section of the continuous flow quartz reactor and of the tubular $\beta''$-$Al_2O_3$ element showing the location of the Ag catalyst (working electrode WE) and of the Au counter (CE) and reference (RE) electrodes.

**TABLE 1**

**Ag Catalyst Surface Areas**

| Catalyst film | Reactive oxygen uptake ($N_O$/mol O) |
|---|---|
| 1 | $4.8 \times 10^{-6}$ |
| 2 | $4.0 \times 10^{-5}$ |
| 3 | $2.9 \times 10^{-5}$ |

22-201), followed by drying and calcining in air, first at 400°C for 2 h and then at 550°C for 2 h. Catalyst preparation and characterization details have been presented elsewhere (34, 43–47). The Au counter and reference electrodes were deposited on the inside walls of the $\beta''$-$Al_2O_3$ tube by application of thin coatings of a Demetron M-8032 gold paste calcined at 800°C for 10 min. The superficial surface areas of the working, counter, and reference electrodes were 8 $cm^2$, 5.5 $cm^2$, and 0.5 $cm^2$, respectively.

It is worth noting that when using a single pellet reactor (34, 49) for NEMCA studies, the "reference" is, strictly speaking, a pseudoreference electrode. This is because in this design the reference electrode is exposed to the same gas mixture as the working electrode and thus its potential is not pinned to a thermodynamically well-defined value. As discussed at the end of this section this is not a serious drawback since only changes in potential, and thus work function (25, 34), values, not absolute values vs a thermodynamically well-established reference, are necessary for the description of the observed phenomena.

Three Ag catalyst films were used in the present investigation and all three gave very similar results. The true surface areas of these three Ag catalyst films, labeled 1, 2, and 3 (Table 1), were measured via the isothermal surface titration technique (28, 47), i.e., by measuring the reactive oxygen uptake of the Ag film via oxygen titration with ethylene at 350°C (28, 47). The inertness of the Au electrodes was verified with blank experiments for the conditions employed in the present study, both under open and closed circuit conditions. On the basis of the measured Ag catalyst surface areas it is possible to compute turnover frequencies (TOFs) for the epoxidation and complete oxidation. Measured TOFs at temperatures 250–300°C in absence of $C_2H_4Cl_2$ were in the order of $10^{-3}$ $s^{-1}$, in good qualitative agreement with literature (51, 52). In the presence of $C_2H_4Cl_2$, however, both TOFs are reduced by up to two orders of magnitude.

Three Au wires attached mechanically to the three electrodes were inserted into the quartz reactor through an appropriately machined Teflon component which was screwed into a water cooled stainless steel cap. An O-ring system was used to provide sealing of the quartz reactor which for safety reasons was inserted in a stainless steel tube also suitably screwed into the steel reactor cup.

The reactor was checked for the absence of internal and external mass transfer limitations under the conditions of the experiments according to the procedure described in earlier works (43, 45). It behaved as a CSTR in the flow range 30–40 $cm^3$ STP/min used in this investigation, as shown by determination of its residence time distribution using the IR $CO_2$ analyzer (43, 45). The conversion of the reactants under open- or closed-circuit conditions was kept below 5%; i.e., the reactor was operated differentially. The rate of ethylene oxide oxidation was thus kept to negligible levels (51).

Constant currents between the catalyst and the counter electrode (galvanostatic operation) or constant potentials between the catalyst and the reference electrode (potentiostatic operation) were applied using a HEKA PG 284 galvanostat–potentiostat. The catalyst overpotential $\eta$ is defined from

$$\eta = V_{WR} - V^o_{WR}, \qquad [2]$$

where $V_{WR}$ is the ohmic-drop-free catalyst potential, i.e., the catalyst potential $V'_{WR}$ relative to the pseudoreference electrode minus the corresponding parasitic ohmic component (34, 54), and $V^o_{WR}$, is the open-circuit catalyst potential value ($I = 0$, $V^o_{WR} = V_{WR(I=0)}$). The parasitic ohmic component was measured using the current interruption technique (34, 54) and was found to be negligible (<10 mV) in all cases.

Since the Au counterelectrode is not in contact with a source of Na, electrochemical supply of sodium onto the Ag catalyst surface results in a small and local depletion of $Na^+$ in the $\beta''$-$Al_2O_3$ lattice in the vicinity of the counterelectrode. These $Na^+$ are replaced by protons (29). Due to the small magnitude of applied current and reversed current application, Na depletion at the counterelectrode does not cause any practical problems and the system remains reversible for many weeks of operation as in previous $\beta''$-$Al_2O_3$ NEMCA studies (25, 28, 29, 31).

Previous *in situ* Kelvin probe measurements (25, 55) of the work function $e\Phi$ of metal electrodes such as Ag, deposited on solid electrolytes such as $\beta''$-$Al_2O_3$, have shown that any change in catalyst potential $V_{WR}$ is accompanied by a concomitant change $\Delta(e\Phi)$ in the catalyst surface work function:

$$\Delta(e\Phi) = e\Delta V_{WR} \qquad [3]$$

The theoretical derivation of Eq. [3] is straightforward and has been presented elsewhere (34, 36, 37).

*Reference and Pseudoreference Electrodes*

Strictly speaking Eq. [3] is exactly valid when a true reference electrode is used. True reference electrodes require the presence of at least one electroactive species with a defined activity in a fluid or solid phase. For example, in NEMCA cells with oxide ion conductors (23–25, 27, 30, 32) a porous nonpolarizable (high exchange current $I_0$) Pt electrode

exposed to oxygen or air can serve as a true reference electrode (34). Its potential, unperturbed by the passage of a small amount of current across it, is pinned to a fixed value via the equilibrium between $O^{2-}$ in the solid electrolyte and gaseous $O_2$, at a well defined partial pressure. If, instead the reference electrode is exposed to the same gas mixture as the working electrode (32) then it can still act as a true reference only to the extent that no reaction is catalyzed on its surface and that the potential-setting charge transfer reaction is still the one between $O^{2-}$ in the solid electrolyte and gaseous $O_2$. Gold electrodes may satisfy these criteria to a satisfactory extent (32).

In NEMCA cells with $Na^+$ conductors (25, 28, 29, 31) a true reference electrode should be in contact with molten Na or a suitable Na alloy of known Na activity. Such a design is not very practical and has not been used yet. Earlier NEMCA studies with $\beta''$-$Al_2O_3$ (25, 28) used a Pt film exposed to ambient air as the reference electrode. This would be a true reference electrode if the sodium activity, or at least coverage, on its surface were exactly known. Since this was not the case (25, 28) these electrodes must be termed pseudoreference electrodes. Their potential is pinned to a fixed, yet thermodynamically not well-defined, value. This is, however, no serious drawback of these earlier NEMCA studies since only changes in the catalyst potential $V_{WR}$ and work function $e\Phi$ are of catalytic interest. This is also the case in the present study where the single pellet design (34, 49) is used and thus the pseudoreference electrode is exposed to the same gas mixture as the catalyst electrode. In order to meet the inertness requirement, Au was chosen as the reference material as in previous studies utilizing the single pellet design with YSZ (32, 49) and $\beta''$-$Al_2O_3$ (29, 50) solid electrolytes. The exact, low (29), coverage of Na on the Au electrode is again not precisely known, but even if it were known, changing the gaseous composition can be expected to lead to changes in the state of sodium on the Au surface, thus in the pseudoreference electrode work function and potential. The extent of such variations in the potential of the pseudoreference electrode is expected to be small and of the order of 0.1 V as can be inferred by comparing the NEMCA results obtained for $C_2H_4$ oxidation on Pt/$\beta''$-$Al_2O_3$ (28, 50) when using a pseudoreference electrode exposed to air (28) and a Au pseudoreference electrode exposed to the reacting gas mixture (50): The sharp decrease in catalytic rate with decreasing potential occurs over practically the same $V_{WR}$ values range (28, 50). It may thus be concluded that the use of Au as a pseudoreference electrode in NEMCA studies utilizing the single pellet design is a practical and adequate choice.

## RESULTS

### *Transients*

Figures 2a and 2b show a typical galvanostatic transient, i.e., a typical catalytic rate, selectivity and catalyst potential response upon imposition of a negative current $I$ of $-10\,\mu$A between the catalyst and the counterelectrode. In this way

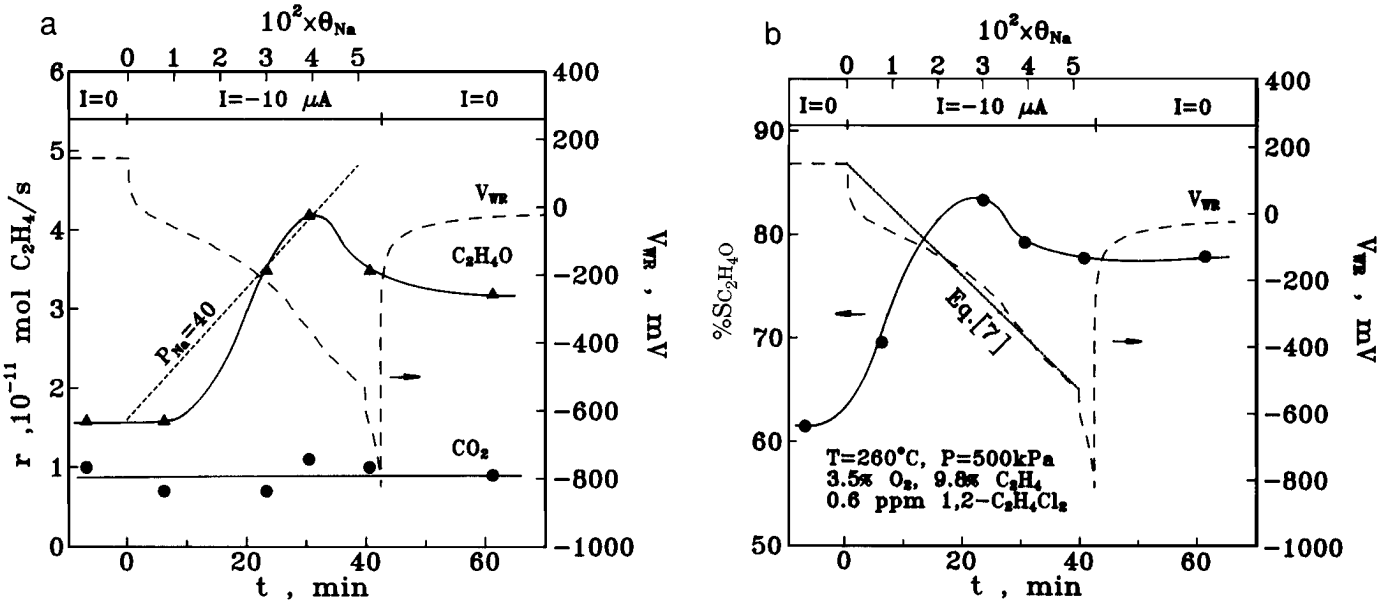


**FIG. 2.** (a) Transient effect of constant applied current and corresponding Na coverage on the rates of ethylene oxide (▲) and $CO_2$ (●) formation and on catalyst potential $V_{WR}$ (broken line). The dotted line labeled $P_{Na}=40$ is constant promotion index line. Total pressure, 500 kPa; 0.6 ppm 1,2-dichloroethane; $P_{O_2}=17.5$ kPa; $P_{C_2H_4}=49$ kPa; $T=260$°C catalyst 1 (see text for discussion). (b) Transient effect of constant applied current on the selectivity to ethylene oxide (●) and on catalyst potential. The dotted line marked Eq. [7] corresponds via Eq. [7] to a Na dipole moment of 2.57 Debye; conditions as in Fig. 2a.

sodium ions are supplied to the Ag catalyst at a constant rate $-I/F$.

The experiment was carried out in the presence of 0.6 ppm of 1,2-$C_2H_4Cl_2$ in the gas phase. Before starting the experiment, residual sodium was removed from the catalyst surface by applying a constant potential of $+400$ mV between the catalyst and the reference electrode for 10 min. The circuit was subsequently opened and the system was left to rest, so that the catalytic rates and catalyst potential attained constant, steady-state values.

Thus at the start of the experiment ($t \le 0$, Fig. 2a) the electrical circuit is open, the open-circuit catalyst potential is $V^o_{WR} = 160$ mV, and the rates of epoxidation and deep oxidation are $r_{0,C_2H_4O} = 1.6 \times 10^{-11}$ mol $C_2H_4$/s and $r_{o,CO_2} = 1.0 \times 10^{-11}$ mol $C_2H_4$/s, respectively. The corresponding open-circuit selectivity to epoxide is $S_o = 62.0\%$ (Fig. 2b). At $t = 0$ the galvanostat is used to apply a constant current $I = -10\ \mu$A between the counterelectrode and the catalyst with a concomitant rate of sodium ion $Na^+$ transfer to the catalyst equal to $(-I/F) = 1.0 \times 10^{-10}$ mol/s via the following electrochemical charge transfer reaction which takes place at the three-phase-boundaries $\beta''$-$Al_2O_3$/Ag/gas of the Ag catalyst electrode,

$$Na^+(\beta''\text{-}Al_2O_3) + e^- \rightleftharpoons Na^{(\delta+)} - Ag^{\delta-}, \qquad [4]$$

where $\delta^-$ stands for the compensating (screening) charge on the Ag surface which accompanies the partially charged $Na^{\delta+}$ species adsorbed on the catalyst surface (34, 36).

As shown on Fig. 2a the complete oxidation rate remains constant while the epoxidation rate starts increasing, goes through a maximum in approximately 30 min, and reaches a new steady-state value of $3.3 \times 10^{-11}$ mol $C_2H_4$/s, i.e., 110% higher than its value before current application. As discussed below this value also remains practically constant after current interruption. At the same time the catalyst potential decreases in a complex manner which reflects not only the increase of sodium coverage but also probably the formation of sodium compounds such as NaOH, $Na_2CO_3$, and sodium oxychloride complexes on the catalyst surface (28, 31, 56). The selectivity to $C_2H_4O$ exhibits the same behavior as the epoxidation rate. As shown on Fig. 2b, the selectivity increases significantly after current application, reaches a maximum value of 83% and stabilizes to a steady-state value of 78%, i.e., 26% higher than its open-circuit value.

The second abscissa axis in Figs. 2a and 2b shows the sodium coverage on the catalyst surface during the transient. This total sodium coverage scale is constructed using the integrated mass balance equation for sodium,

$$\theta_{Na^{\delta+}} = -It/FN_O, \qquad [5]$$

where $N_O = 4.8 \times 10^{-6}$ mol Ag is the surface area of the Ag catalyst film obtained by measuring its reactive oxygen uptake via the isothermal surface titration technique (28, 47) and assuming a 1 : 1 Ag to O stoichiometry (47). Equation [5] is derived by taking into account that at $t = 0$ the sodium coverage on the silver catalyst surface is zero. As shown on Fig. 2b the maximum in selectivity to epoxide corresponds to a sodium coverage of 0.03.

Upon current interruption the catalyst potential starts increasing (Figs. 2a, 2b). In accordance with the behavior observed in previous NEMCA studies utilizing $\beta''$-$Al_2O_3$ (25, 28, 29, 31), the catalytic rates do not change appreciably upon current interruption since $Na^{\delta+}$ cannot be scavenged from the catalyst surface. Potentiostatic imposition of the initial catalyst potential for several minutes, i.e., until the current practically vanishes, was found to be necessary in order to restore the catalytic rates to their initial values, as in all previous NEMCA studies utilizing $\beta''$-$Al_2O_3$ (25, 28, 29, 31).

Since a change $\Delta V_{WR}$ in catalyst potential corresponds to a change $\Delta(e\Phi)$ in the work function of the gas exposed catalyst surface equal to $e\Delta V_{WR}$ (Eq. [3]) one can use the definition of $\theta_{Na}$, Faraday's law, and the differentiated Helmholtz equation (28, 29, 34, 57) to obtain (28, 29, 34)

$$\frac{edV_{WR}}{dt} = \frac{d(e\Phi)}{dt} = \frac{P'_{Na}I}{\varepsilon_o A}, \qquad [6]$$

where $\varepsilon_0 = 8.85 \times 10^{-12}$ C$^2$/(J · m), $P'_{Na}$ is the dipole moment of sodium on Ag, and $A$ is the total catalyst surface area (0.21 m$^2$, computed from $N_O = 4.8 \times 10^{-6}$ mol Ag and the surface atom density of Ag(111), $N_{Ag} = 1.38 \times 10^{19}$ atom/m$^2$).

Equation [6] can thus be used in conjunction with the $V_{WR}$ transient in Fig. 2a (or 2b) to estimate the average dipole moment $P'_{Na}$ of sodium on the Ag catalyst surface. If $P'_{Na}$ were independent of Na coverage, then $V_{WR}$ would decrease linearly with $t$ in the transient experiment of Fig. 2. The fact that the $V_{WR}$ decrease is more complex (Fig. 2) shows that $P'_{Na}$ depends on the sodium coverage $\theta_{Na}$, as is the case even for atomically clean surfaces under UHV conditions (57). In the present case the situation is more complex due to the coadsorption of oxygen, ethylene, and chlorine and the formation of sodium compounds on the surface (31). Nevertheless, one can use the $V_{WR}$ transient (Fig. 2) in conjunction with Eq. [6] to compute an average value, $\bar{P}'_{Na}$, for the dipole moment of sodium on the catalyst surface (dotted line marked Eq. [7] on Fig. 2b). The computed value of $0.85 \times 10^{-29}$ C · m ($= 2.57$ Debye) is very reasonable. It is 50% smaller than the initial dipole moment of sodium on polycrystalline Pt and Pt(111) (28, 29, 57) and within 20% of that on Ni(100) and Ru(0001) (57, 58).

The exact $\Delta V_{WR}$, and $\Delta(e\Phi)$, vs $\theta_{Na}$ relationship is nonlinear and depends to a certain extent on the surface coverages of oxygen, ethylene, and chlorine (29). Despite this complication we have chosen for a more simplified presentation, to show additionally in subsequent figures an approximate

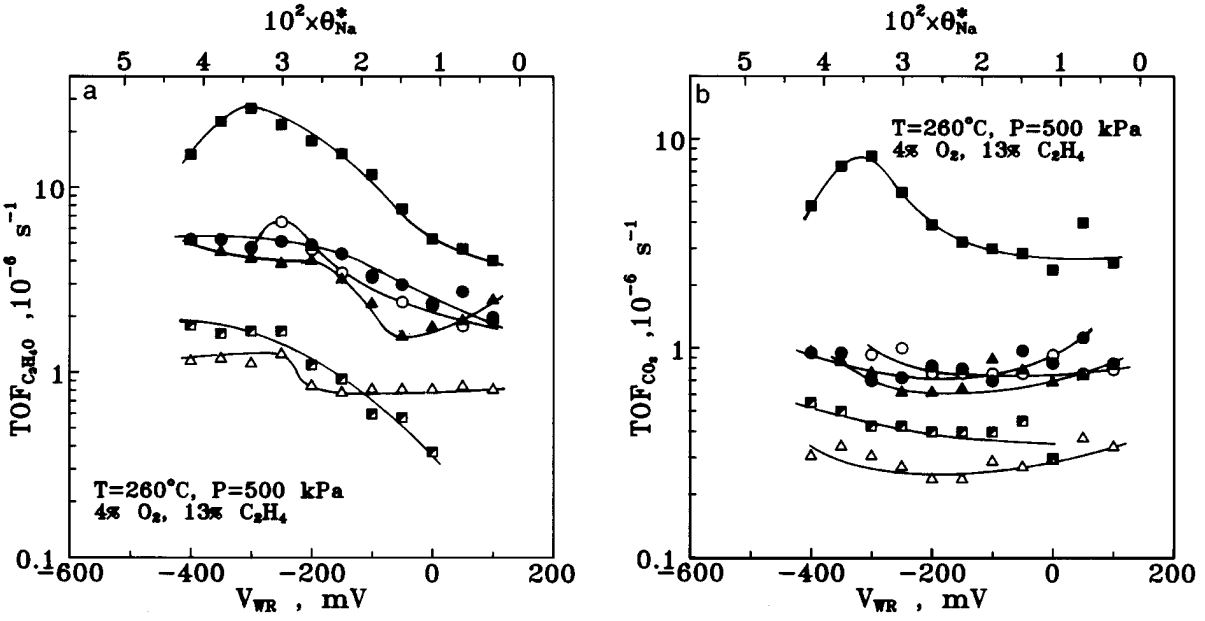


**FIG. 3.** Steady-state effect of catalyst potential, $V_{WR}$, and corresponding linearized Na coverage, $\theta^*_{Na}$, on the turnover frequency (TOF) (molecules ethylene reacting to epoxide or $CO_2$ per surface Ag atom per second) of ethylene epoxidation (a) and complete oxidation (b) at various levels of addition of dichloroethane. Closed symbols, catalyst 2: (■) 0.4 ppm $C_2H_4Cl_2$, (●) 1.0 ppm $C_2H_4Cl_2$, (▲) 1.3 ppm $C_2H_4Cl_2$, (◩) 1.6 ppm $C_2H_4Cl_2$. Open symbols, catalyst 3: (○) 1.0 ppm $C_2H_4Cl_2$, (△) 2.0 ppm $C_2H_4Cl_2$.

linear Na coverage scale, labeled hereafter $\theta^*_{Na}$ to distinguish it from the precisely measured (coulometrically) Na coverage $\theta_{Na}$ shown in Figs. 2a and 2b. This linear approximate scale is constructed via the Helmholz equation,

$$\theta^*_{Na} = -\varepsilon_o \Delta(e\Phi)/(e\bar{P}'_{Na} N_{Ag}), \qquad [7]$$

using the above average $\bar{P}'_{Na}$ value. Substituting the numerical values in Eq. [7] one obtains

$$\theta^*_{Na} = -0.076\Delta(e\Phi/eV). \qquad [8]$$

The deviation of $\theta^*_{Na}$ from the actual $\theta_{Na}$ for any given $\Delta(e\Phi)$ value is typically less than 30% as can be inferred from Fig. 2b.

*Steady State Behavior*

*Effect of catalyst potential $V_{WR}$.* Figure 3 shows the steady-state effect of catalyst potential and corresponding linearized sodium coverage, $\theta^*_{Na}$, on the rates of epoxidation and complete oxidation for various concentrations of 1,2-$C_2H_4Cl_2$ in the gas phase and for two different catalyst films. All steady-state kinetic results reported here were stable over periods of several hours. No longer term investigation of rate and selectivity stability was performed.

As shown in Fig. 3, the $CO_2$ production rate is, in general, very little affected by catalyst potential and sodium coverage, whereas the epoxidation rate is enhanced with decreasing catalyst potential, i.e., increasing sodium coverage. In the case of low $C_2H_4Cl_2$ concentrations the rate of epoxidation goes through a maximum at $V_{WR} = -250$ to $-300$ mV. The observed rate behavior results in a substantial increase in the selectivity to $C_2H_4O$ with decreasing catalyst potential or, equivalently, catalyst work function, up to a certain potential value ($-150$ to $-300$ mV) below which the selectivity is slightly decreased (Figs. 4a and 4b). The global maximum selectivity value for both films was 88% in the presence of 1.0 ppm of 1,2-$C_2H_4Cl_2$ in the gas phase and $V_{WR} = -250$ mV corresponding to a sodium coverage of 0.03.

As analyzed below the observed selectivity behavior is due to the stabilization of adsorbed chlorine on the catalyst surface with increasing sodium coverage which favors the creation of weakly adsorbed electrophilic oxygen atoms.

*Effect of gas-phase addition of 1,2-$C_2H_4Cl_2$.* As shown in Fig. 3 the addition of traces of 1,2-$C_2H_4Cl_2$ in the feed reduces drastically the catalytic activity both for epoxidation and for complete oxidation of ethylene. This is due to the reduction of atomic oxygen coverage as chlorine is adsorbed competitively with oxygen on the silver catalyst surface (4). On the other hand, the adsorption of chlorine enhances up to a certain point the selectivity to $C_2H_4O$ (Figs. 4a and 4b) as it weakens the bond strength of coadsorbed oxygen via electron backdonation from the metal, thus creating weakly bound electrophilic oxygen atoms (4). The dependence of the selectivity to $C_2H_4O$ on 1,2-$C_2H_4Cl_2$ concentration at various catalyst potentials is shown in Fig. 5. This three-dimensional plot was constructed by fitting a large number of data (~50) at $T = 260°C$, $P_{O_2} = 20$ kPa, and

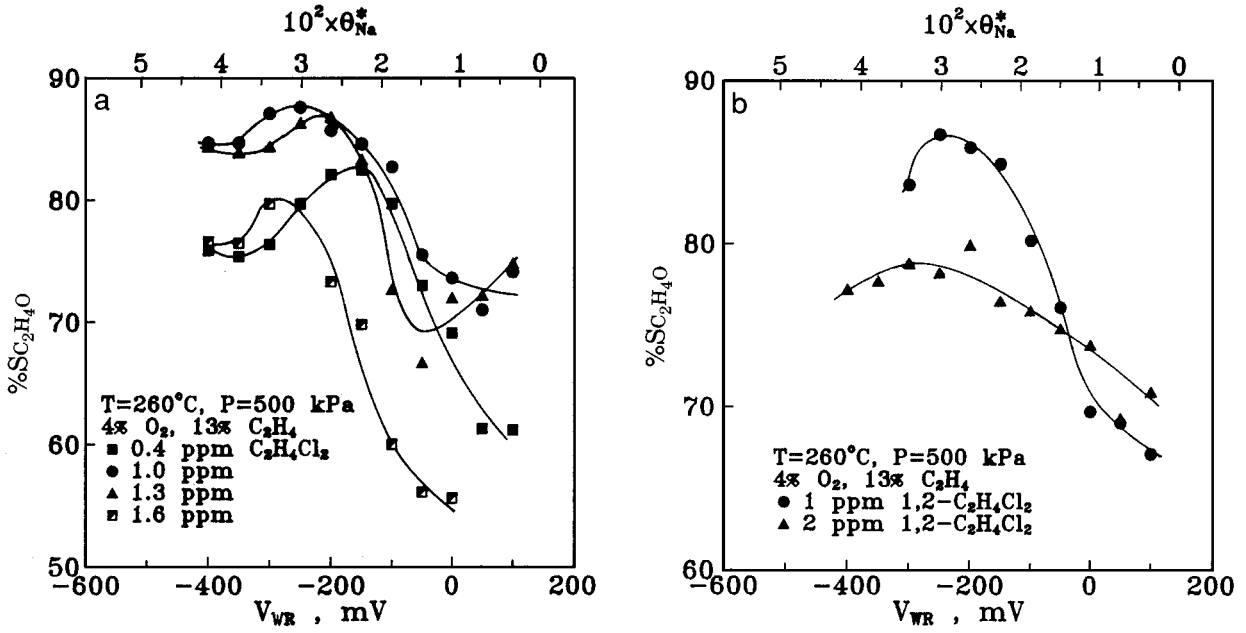


**FIG. 4.** Steady-state effect of catalyst potential on the selectivity to ethylene oxide at various levels of gas-phase dicloroethane: (a) catalyst 2, (b) catalyst 3.

$P_{C_2H_4} = 65$ kPa to a polynomial expression. Fig. 5 shows that the selectivity goes through a maximum with respect to both dichloroethane concentration and catalyst potential. This maximum occurs at $P_{C_2H_4Cl_2} = 1$ ppm, $V_{WR} = -250$ mV; thus, $\theta_{Na} = 0.03$.

As shown in Fig. 5, and also manifested in Figs. 4a and 4b, for each concentration of dichloroethane there is an optimal $V_{WR}$ value, denoted $V_{WR,\,opt}$ which maximizes the selectivity. Figure 6 shows the dependence of the selectivity on dichloroethane concentration at $V_{WR,\,opt}$, whereas Fig. 7 shows the $V_{WR,\,opt}$ dependence on dichloroethane concentration. It is noteworthy that the data obtained with the two different Ag catalyst films fall on the same curves (Figs. 6 and 7).

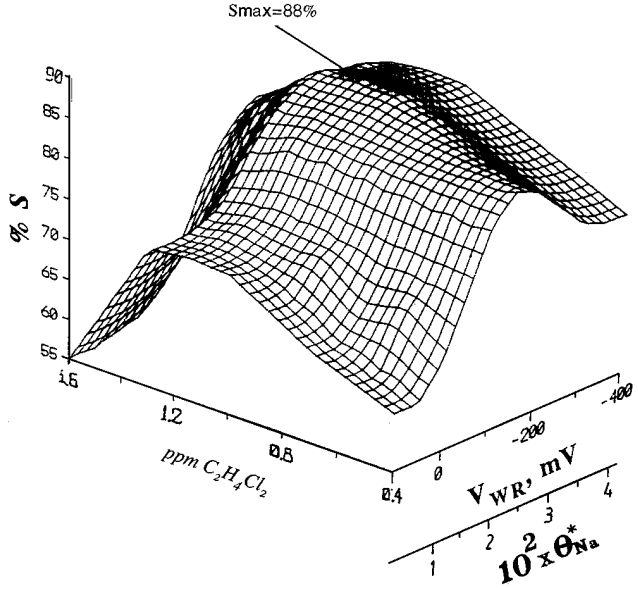


**FIG. 5.** Steady-state effect of dichloroethane concentration, catalyst potential, and corresponding linearized Na coverage on the selectivity to ethylene oxide. $T = 260°C$, $P_{O_2} = 20$ kPa, $P_{C_2H_4} = 65$ kPa; catalyst 2.

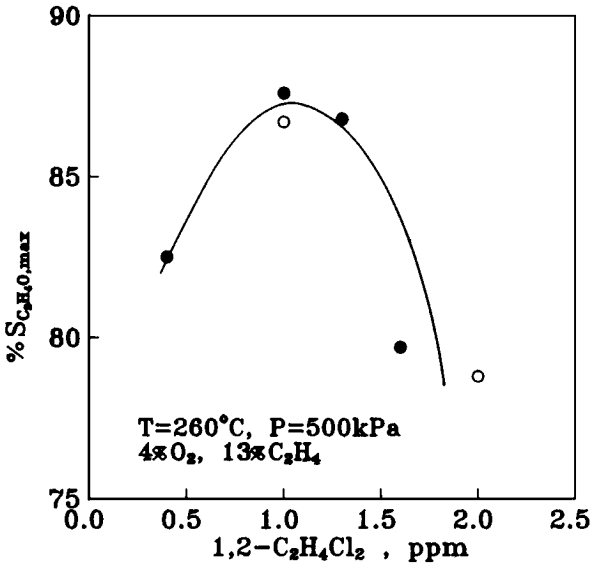


**FIG. 6.** Effect of dichloroethane concentration on the maximum obtainable selectivity to ethylene oxide via variation in catalyst potential, i.e., at $V_{WR,\,opt}$. (●) Catalyst 2, (○) catalyst 3.

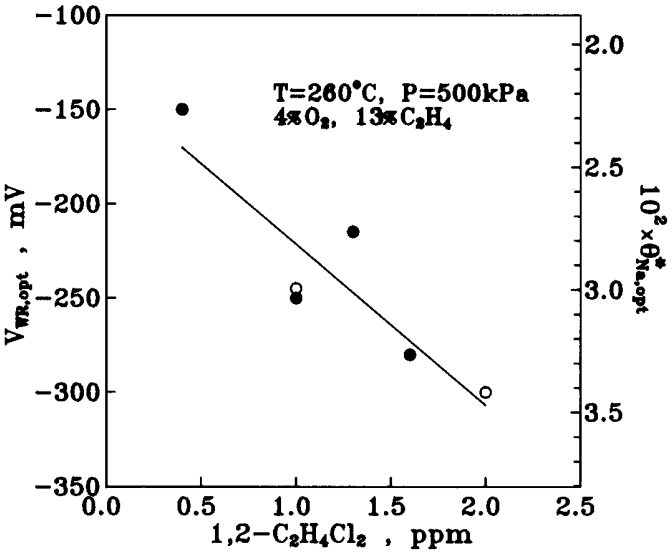


**FIG. 7.** Effect of dichloroethane concentration on the optimal catalyst potential, $V_{WR,opt}$, and corresponding optimal Na coverage, $\theta_{Na,opt}$, for selectivity maximization. (●) Catalyst 2, (○) catalyst 3.

Figure 7 shows that increasing Cl coverage on the surface requires a correspondingly higher Na coverage to yield maximum selectivity. This shows clearly the synergistic promotional role of Na and Cl for ethylene epoxidation. Interestingly, the dependence of $V_{WR,opt}$ (thus also optimal Na coverage) on dichloroethane concentration is linear (Fig. 7).

## DISCUSSION

The present results show that $\beta''$-$Al_2O_3$ can be used as an active catalyst support to significantly affect the catalytic properties of Ag for the epoxidation of ethylene. Alkali promoters are used in industry, along with chlorine compounds in the gas phase, to enhance the selectivity to $C_2H_4O$. The use of $\beta''$-$Al_2O_3$ offers the possibility of controlling *in situ* and in a reversible manner the sodium coverage on silver catalysts interfaced with $\beta''$-$Al_2O_3$, by applying appropriate potentials between the silver catalyst and a reference electrode, and thus of studying *in situ* the promotional role of sodium.

Values of the promotion index (27, 29), defined from

$$P_i = \frac{\Delta r / r_o}{\theta_{Na}}, \qquad [1]$$

as high as 40 were measured in the present work for the epoxidation reaction (Fig. 2a), which shows the strong promotional effect of sodium for this reaction.

Under the conditions studied in the present work both the sodium coverage, i.e., the catalyst potential, and the 1,2-$C_2H_4Cl_2$ concentration play important roles in determining the selectivity to ethylene oxide.

The effect of chlorine coadsorption seems twofold: First chlorine atoms replace strongly adsorbed oxygen atoms, as they compete with them for the same sites (3, 4). Second, chlorine adsorption weakens the bond strength of coadsorbed oxygen by withdrawal of electrons from the silver atoms and by creation of sites for the adsorption of weakly bound electrophilic oxygen (3–5) which interacts with the double bond of ethylene molecule producing $C_2H_4O$ (4). On the other hand, the presence of sodium on the silver surface seems to stabilize the adsorbed chlorine (Fig. 7) via the formation of a silver-oxychloride surface complex (4, 56).

The present results can be explained by the above considerations. As shown on Fig. 3, the catalytic rates decrease with increasing concentration of 1,2-$C_2H_4Cl_2$ in the gas phase, as chlorine adsorption reduces the number of sites available for oxygen adsorption. The observed increase in the epoxidation rate (Figs. 2a, 3a) and in selectivity to $C_2H_4O$ (Figs. 2b, 4a, and 4b) with decreasing catalyst potential, i.e., increasing sodium coverage, shows that (electropositive) sodium addition mitigates the reduction of epoxidation rate induced by chlorine, without notably affecting the chlorine-induced suppression in the complete oxidation rate. These observations show that the right combined concentrations of chlorine and sodium lead to the stabilization of the silver-oxychloride surface complex (4, 56) and thus to higher coverages of weakly bound oxygen, leading to epoxidation, and lower coverages of strongly bound oxygen, leading to complete oxidation (4, 56).

The observed decrease in selectivity to $C_2H_4O$ at very negative catalyst potentials (Figs. 4a, 4b) must result from the pronounced decrease in the work function of the catalyst surface (Fig. 2) and from the concomitant increase (Fig. 5) of the silver–oxygen bond strength (44–47, 59). This increases the coverage of the strongly bonded ionic oxygen atoms which react preferentially with the hydrogen atoms of ethylene and produce $CO_2$ via C–H bond rupture.

The observed maximum in the selectivity to $C_2H_4O$ with respect to the gas-phase concentration of 1,2-$C_2H_4Cl_2$ (Figs. 4, 5, 6) must result from the fact that at very high coverages of adsorbed chlorine, which in general were found to increase the catalyst work function by up to 0.2 eV (46, 48), the binding energy of adsorbed ethylene increases significantly via enhanced $\pi$-electron donation (4, 34, 46). Strongly adsorbed ethylene is preferentially oxidized completely and thus the selectivity to ethylene oxide decreases (Fig. 5).

The maximum selectivity value of 88% obtained in the present study is one of the highest values reported in the open or patent literature. Thus, the results may be of technological importance. The present work demonstrates the usefulness of solid electrolytes as active catalyst supports in influencing product selectivity in desired directions via the NEMCA effect and in studying *in situ* the role of promoters.

## ACKNOWLEDGMENTS

We thank the EEC SCIENCE, HCM, and JOULE programmes for financial support and our reviewers for some thoughtful comments.

## REFERENCES

1. Kilty, P. A., and Sachtler, W. H., *Catal. Rev. Sci. Eng.* **10**, 1 (1974).
2. Verykios, X. E., Stein, F. P., and Coughlin, R. W., *Cat. Rev. Sci. Eng.* **22**, 197 (1980).
3. Sachtler, W. M. H., Backx, C., and Van Santen, R. A., *Catal. Rev. Sci. Eng.* **23**, 127 (1981).
4. Van Santen, R. A., and Kuipers, H. P. C. E., *in* "Advances in Catalysis" (D. D. Eley, H. Pines and P. B. Weisz, Eds.), Vol. 35, p. 265. Academic Press, New York, 1987.
5. Rovida, G., Pratesi, G., and Ferroni, E., *J. Catal.* **41**, 140 (1976).
6. Spencer, N. D., and Lambert, R. M., *Chem. Phys. Lett.* **83**, 388 (1981).
7. Kitson, M., and Lambert, R. M., *Surf. Sci.* **109**, 60 (1981).
8. Kitson, M., and Lambert, R. M., *Surf. Sci.* **110**, 205 (1981).
9. Peuckert, M., *Surf. Sci.* **146**, 329 (1984).
10. Tan, S. A., Grant, R. B., and Lambert, R. M., *J. Catal.* **106**, 54 (1987).
11. Campbell, C. T., *J. Catal.* **99**, 28 (1986).
12. Dean, M., and Bowker, M., *J. Catal.* **115**, 138 (1989).
13. Grant, R. B., and Lambert, R. M., *J. Catal.* **92**, 364 (1985).
14. Tan, S. A., Grant, R. B., and Lambert, R. M., *J. Catal.* **104**, 156 (1987).
15. Backx, C., De Groot, C. P. M., and Biloen, P., *Surf. Sci.* **104**, 300 (1981).
16. Campbell, C. C., and Paffett, M. T., *Surf. Sci.* **143**, 517 (1984).
17. Rehren, C., Muhler, M., Bao, X., Schlögl, R., and Ertl, G., *Z. Phys. Chem,* **174**, 11 (1991).
18. Van den Hoek, P. J., Baerends, E. J., and Van Santen, R. A., *J. Phys. Chem.* **93**, 6469 (1989).
19. Gleaves, J. T., Sault, A. G., Madix, T. J., and Ebner, J. R., *J. Catal.* **121**, 202 (1990).
20. Van Santen, R. A., and De Groot, C. P. M., *J. Catal.* **98**, 530 (1980).
21. Bukhtiyarov, V. I., Boronin, A. I., and Savchenko, V. I., *J. Catal.* **150**, 262 (1994); *J. Catal.* **150**, 268 (1994).
22. Jørgensen, K. A., and Hoffmann, R., *J. Phys. Chem.* **94**, 3046 (1990).
23. Vayenas, C. G., Bebelis, S., and Neophytides, S., *J. Phys. Chem.* **92**, 5083 (1988).
24. Bebelis, S., and Vayenas, C. G., *J. Catal.* **118**, 125 (1989).
25. Vayenas, C. G., Bebelis, S., and Ladas, S., *Nature (London)* **343**, 625 (1990).
26. Politova, T. I., Sobyanin, V. A., and Belyaev, V. D., *React. Kinet. Catal. Lett.* **41**, 321 (1990).
27. Pliangos, C., Yentekakis, I. V., Verykios, X. E., and Vayenas, C. G., *J. Catal.* **154**, 124 (1995).
28. Vayenas, C. G., Bebelis, S., and Despotopoulou, M., *J. Catal.* **128**, 415 (1991).
29. Yentekakis, I. V., Moggridge, G., Vayenas, C. G., and Lambert, R. M., *J. Catal.* **146**, 292 (1994).
30. Varkaraki, E., Nicole, J., Plattner, E., Comninellis, Ch., and Vayenas, C. G., *J. Appl. Electrochem.* **25**, 978 (1995).
31. Harkness, I. R., and Lambert, R. M., *J. Catal.* **152**, 211 (1995).
32. Cavalca, C. A., Larsen, G., Vayenas, C. G., and Haller, G. L., *J. Phys. Chem.* **97**, 6115 (1993).
33. Cavalca, C. A., and Haller, G. L., *J. Catal.,* in press (1996).
34. Vayenas, C. G., Bebelis, S., Yentekakis, I. V., Lintz, H.-G., *Catal. Today* **11**, 303 (1992).
35. Vayenas, C. G., Ladas, S., Bebelis, S., Yentekakis, I. V., Neophytides, S., Jiang Yi, Karavasilis, Ch., and Pliangos, C., *Electrochim. Acta* **39**(11/12), 1849 (1994).
36. Vayenas, C. G., Jaksic, M. M., Bebelis, S. I., and Neophytides, S. G., The Electrochemical activation of catalytic reactions *in* "Modern Aspects of Electrochemistry" (J. O. 'M. Bockris *et al.*, Eds.), Vol. 29, p. 57. Plenum, New York, 1995.
37. Vayenas, C. G., and Yentekakis, I. V., Electrochemical modification of catalytic activity, in "Handbook of Heterogeneous Catalysis" (G. Ertl, H. Knötzinger, and J. Weitkamp, Eds.). VCH, Weinheim, New York, in press, 1996.
38. Neophytides, S. G., Tsiplakides, D., Stonehart, P., Jaksic, M. M., and Vayenas, C. G., *Nature* (London), **370**, 45 (1994).
39. Ladas, S., Kennou, S., Bebelis, S., and Vayenas, C. G., *J. Phys. Chem.* **97**, 8845 (1993).
40. Pritchard, J., *Nature* (London) **342**, 592 (1990).
41. Bockris, J. O. 'M., and Minevski, Z. S., *Electrochem. Acta* **39**(**11/12**), 1471 (1994).
42. Lamy-Pitara, E., Bencharif, L., and Barbier, J., *Appl. Catal.* **18**, 117 (1985).
43. Stoukides, M., and Vayenas, C. G., *J. Catal.* **70**, 137 (1981).
44. Stoukides, M., and Vayenas, C. G., *ACS Symp. Ser.* **178**, 181 (1982).
45. Bebelis, S., and Vayenas, C. G., *J. Catal.* **138**, 588 (1992).
46. Karavasilis, Ch., Bebelis, S., and Vayenas, C. G., *J. Catal.*, **160**, 190 (1996).
47. Bebelis, S., and Vayenas, C. G., *J. Cat.* **138**, 570 (1992).
48. Karavasilis, Ch., Ph.D. thesis, University of Patras (1994).
49. Yentekakis, I. V., and Bebelis, S., *J. Catal.*, **137**, 278 (1992).
50. Harkness, I. R., Hardacre, C., Lambert, R. M., Yentekakis, I. V., and Vayenas, C. G., *J. Catal.,* in press (1996).
51. Stoukides, M., and Vayenas, C. G., *J. Catal.* **82**, 45 (1983).
52. Seyedmonir, S. R., Plischke, J. K., Vannice, M. A., and Joung, H. W., *J. Catal.* **123**, 534 (1990).
53. Bockris, J. O. 'M., and Reddy, A. K. N., *in* "Modern Electrochemistry" Vol. 2. Plenum, New York, 1970.
54. Wang, D. Y., and Nowick, A. S., *J. Electrochem. Soc.* **126**, 1155 (1979).
55. Ladas S., Bebelis, S., and Vayenas, C. G., *Surf. Sci.* **251/252**, 1062 (1991).
56. Van Santen, R. A., Proc. of the 9th Int. Congress, on Catalysis, Vol. 3, Calgary (1988) (M. J. Phillips, & M. Tenan, Eds.); *Surface Science* **251/252**, 6 (1991).
57. Hölzl, J., and Schulte, F. K., *in* "Solid Surface Physics," pp. 1–150. Springer Verlag, Berlin, 1979.
58. Kiskinova, M. P., *in* "Poisoning and Promotion in Catalysis Based on Surface Science Concepts and Experiments," Elsevier, Amsterdam, 1992.
59. Boudart, M., *J. Am. Chem. Soc.* **74**, 3556 (1952).